International Journal of
*Molecular Sciences*

MDPI

*Article*

# Starch-Coated Magnetic Iron Oxide Nanoparticles for Affinity Purification of Recombinant Proteins

**Vasilisa V. Krasitskaya [1], Alexander N. Kudryavtsev [1], Roman N. Yaroslavtsev [2,3], Dmitry A. Velikanov [2], Oleg A. Bayukov [2], Yulia V. Gerasimova [2,4], Sergey V. Stolyar [2,3,4] and Ludmila A. Frank [1,4,*]**

1 Institute of Biophysics SB RAS, Federal Research Center "Krasnoyarsk Science Center SB RAS", 660036 Krasnoyarsk, Russia; vasilisa.krasitskaya@gmail.com (V.V.K.); kirush07@mail.ru (A.N.K.)
2 Kirensky Institute of Physics SB RAS, Federal Research Center "Krasnoyarsk Science Center SB RAS", 660036 Krasnoyarsk, Russia; yar-man@bk.ru (R.N.Y.); dpona1@gmail.com (D.A.V.); helg@iph.krasn.ru (O.A.B.); jul@iph.krasn.ru (Y.V.G.); stol@iph.krasn.ru (S.V.S.)
3 Federal Research Center "Krasnoyarsk Science Center SB RAS", 660036 Krasnoyarsk, Russia
4 School of Fundamental Biology and Biotechnology, Siberian Federal University, 660041 Krasnoyarsk, Russia
* Correspondence: lfrank@yandex.ru

**Abstract:** Starch-coated magnetic iron oxide nanoparticles have been synthesized by a simple, fast, and cost-effective co-precipitation method with cornstarch as a stabilizing agent. The structural and magnetic characteristics of the synthesized material have been studied by transmission electron microscopy, Mössbauer spectroscopy, and vibrating sample magnetometry. The nature of bonds between ferrihydrite nanoparticles and a starch shell has been examined by Fourier transform infrared spectroscopy. The data on the magnetic response of the prepared composite particles have been obtained by magnetic measurements. The determined magnetic characteristics make the synthesized material a good candidate for use in magnetic separation. Starch-coated magnetic iron oxide nanoparticles have been tested as an affinity sorbent for one-step purification of several recombinant proteins (cardiac troponin I, survivin, and melanoma inhibitory activity protein) bearing the maltose-binding protein as an auxiliary fragment. It has been shown that, due to the highly specific binding of this fragment to the starch shell, the target fusion protein is selectively immobilized on magnetic nanoparticles and eluted with the maltose solution. The excellent efficiency of column-free purification, high binding capacity of the sorbent (100–500 μg of a recombinant protein per milligram of starch-coated magnetic iron oxide nanoparticles), and reusability of the obtained material have been demonstrated.

**Keywords:** iron oxide nanoparticles; starch; affinity sorbent; maltose-binding protein; hybrid proteins purification



**Citation:** Krasitskaya, V.V.; Kudryavtsev, A.N.; Yaroslavtsev, R.N.; Velikanov, D.A.; Bayukov, O.A.; Gerasimova, Y.V.; Stolyar, S.V.; Frank, L.A. Starch-Coated Magnetic Iron Oxide Nanoparticles for Affinity Purification of Recombinant Proteins. *Int. J. Mol. Sci.* **2022**, *23*, 5410. https://doi.org/10.3390/ijms23105410

Academic Editor: Alexandru Mihai Grumezescu

Received: 15 April 2022
Accepted: 10 May 2022
Published: 12 May 2022



## 1. Introduction

The number of studies on various biomedical and biotechnological applications of magnetic nanoparticles (MNPs) has been steadily increasing [1,2]. Due to the combination of the large specific surface area and unique magnetic properties, MNPs find application in cell separation [3], drug and gene delivery [4], magnetic resonance imaging (MRI) [5], minimally invasive surgery and hyperthermia [6], in vitro molecular diagnostics (biosensing) [7], and are used as affinity sorbents for isolation/pre-concentration of target molecules [8]. In separation and isolation of macromolecules, MNPs work similarly to sorbents of other types (latexes, polymer, and inorganic), but make it possible to use magnetic separation instead of centrifugation, filtration, or chromatography systems and thereby reduce the time of separation of target products and automate the process.

To be used as affinity sorbents, MNPs should meet certain requirements, specifically, to have desired magnetic properties, be resistant against microbes and enzymes, exhibit the "zero" adsorption capacity to prevent nonspecific interactions and the stability of the

functional surface, and contain an immobilized ligand for forming specific complexes with target biomolecules. Among a wide range of MNPs, iron oxide ones were proven to be promising candidates for the role of sorbents, owing to the synthesis simplicity, high magnetization, and superparamagnetism [9]. For use as sorbents, colloidal solutions of MNPs are conventionally prepared. The behavior of nanoparticles in a magnetic field strongly depends on the stability of orientation of their magnetic moments against thermal fluctuations. Superparamagnetic nanoparticles are characterized by the hysteresis-free behavior and high colloidal stability. In the blocked state, nanoparticles exhibit the field hysteresis and high magnetic susceptibility, whereas in a colloid they are less stable. The point between the temperatures of the superparamagnetic and blocked states is called the blocking temperature ($T_B$). This parameter of nanoparticles is important for biomedical applications, including magnetic separation. For use in magnetic separation, the blocking temperature of nanoparticles should be similar to room temperature.

The blocking temperature depends, in particular, on characteristic measurement time $\tau$ [10]. The blocking temperature and the characteristic measurement time are related by the Néel-Brown formula where $K$ is the anisotropy constant, $V$ is the particle volume, $\tau_0$ is the nanoparticle relaxation time, and $k_B$ is the Boltzmann constant.

$$T_B = \frac{KV}{k_B \ln(\tau/\tau_0)}, \quad (1)$$

The characteristic measuring time is ~$10^2$ s for the quasi-static measurements, ~$2.5 \times 10^{-8}$ s for Mössbauer spectroscopy, and ~$10^{-10}$ for X-band ferromagnetic resonance (FMR). Therefore, a method for determining the blocking temperature should be selected according to the field of application of nanoparticles. For example, the blocking temperature of nanoparticles for use in FMR hyperthermia [11,12] should be determined by the FMR method, while the blocking temperature of nanoparticles for magnetic separation [13,14] should be determined by magnetometry.

According to Equation (1), the blocking temperature depends also on the constant of the magnetic anisotropy, which involves three contributions: the magnetocrystalline, surface, and shape anisotropies. The blocking temperature of nanoparticles can be changed by changing their size and shape. The plate-shaped and cubic nanoparticles have a large anisotropy constant and, consequently, a high blocking temperature [15].

Since naked iron oxide MNPs are prone to oxidization and aggregation, different stabilizers and coating agents are used to enhance their stability. In addition, a coating can act as a spacer for attaching certain biomolecules to a magnetic carrier. The materials used for coating MNPs include inorganic compounds (silicon oxide, carbon, and noble metals) and synthetic (PEG, PVA, etc.) and natural (chitosan, polysaccharides, proteins, and peptides) polymers [9]. Different polysaccharides are also frequently used for this purpose due to their chemical and structural diversity, which provides an excellent opportunity to develop novel magnetic micro- or nanocomposites with the high sorption capacity. Various magnetic nanoparticles carrying cellulose, chitosan, arabinogalactan, dextran, and amylose were synthesized and then functionalized with specific biomolecules [16–18].

In this work, starch-coated iron oxide MNPs (starch-MNPs) were synthesized and tested as an affinity sorbent for purifying recombinant proteins genetically fused with maltose-binding protein (MBP), which is a common protein expression tag. This is a 42-kDa single-chain protein encoded by the *E. coli* malE gene [19], which specifically binds to maltose and amylopectin. MBP is widely used as a fusion partner in production of a recombinant protein in bacterial cells to increase the expression level, improve the folding and solubility of the protein of interest [20], and implement its one-step purification on amylose-activated resin. Purification is carried out under the mild elution conditions, which maintain the specific activity of a target protein [21–23]. MNPs were prepared from iron sulfate by a simple co-precipitation method with cornstarch (amylose-amylopectin copolymer) as a stabilizing agent. The method allowed us to synthesize starch-MNPs with

the required magnetic response and dispersibility in aqueous solutions without additional surface functionalization and starch pretreatment stages.

The obtained starch-MNPs were tested as a sorbent for affine purification of several small and medium-sized MBP-fused recombinant proteins: cardiac troponin I (cTnI), a highly specific early biomarker for acute myocardial infarction [24] and survivin (Surv) and melanoma inhibitory activity protein (MIA), the cancer biomarkers of negative prognosis and decreased survival in cancer patients [25,26]. The synthesized starch-MNPs showed excellent purification efficiency, high binding capacity, stability, as well as reusability.

## 2. Results and Discussion

### *2.1. Physical Properties of Starch-MNPs*

The starch-MNPs were prepared by co-precipitation of iron sulfate and cornstarch (21–24% amylose) as a stabilizing agent.

Figure 1 shows high-resolution transmission electron microscopy (HRTEM) images, a microdiffraction pattern, and a size distribution of the starch-MNPs. The particles are cubic nanocrystals with an average size of ~11.5 nm. The microdiffraction pattern (Figure 1b) is characteristic of a spinel structure (magnetite or maghemite).

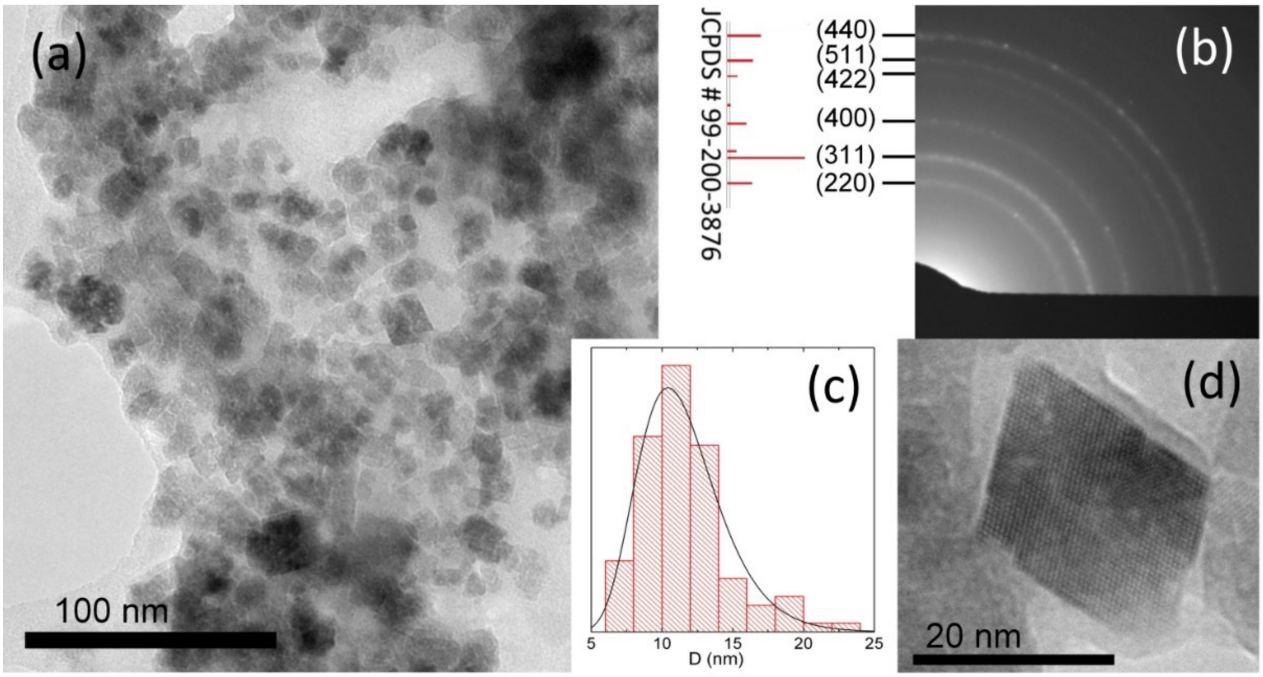


**Figure 1.** HRTEM images at (**a**) the ×100 k and (**d**) ×400 k magnifications, (**b**) microdiffraction pattern, and (**c**) size distribution of the synthesized iron oxide nanoparticles.

The Mössbauer spectrum (Figure 2) shows that all iron ions are in the trivalent state. The experimental spectrum fits well with the components shown. The results of the spectrum interpretation are given in Table 1. The fit error is 3%. Four sextets and one doublet were observed. The widths of 3–4 lines of the inner sextets are extraordinarily large, which is indicative of electron density fluctuations on iron nuclei (variations in chemical shifts on these sites). Therefore, the sample can be identified as extremely defective maghemite. Since only 11% of iron nuclei are characterized by a doublet, i.e., are in the superparamagnetic state, it can be concluded that the average blocking temperature is significantly higher than room temperature.

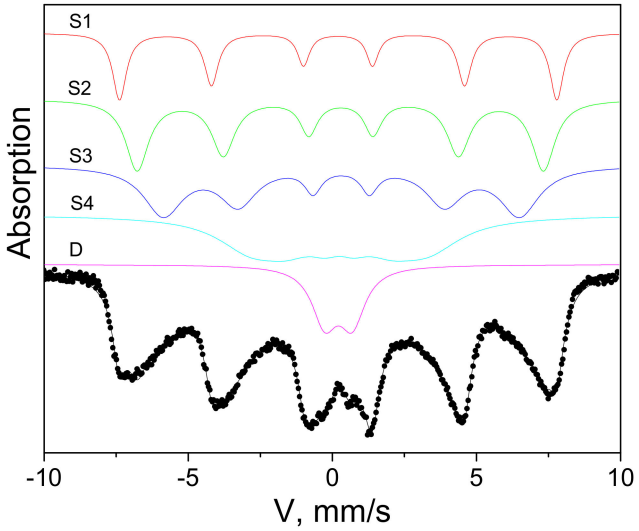


**Figure 2.** Mössbauer spectrum of starch-MNPs.

**Table 1.** Parameters of the Mössbauer spectrum of starch-MNPs.

| IS, mm/s | H, kOe | QS, mm/s | $W_{34}$, mm/s | A, Fract. % | |
|---|---|---|---|---|---|
| 0.34 | 474 | 0.01 | 0.50 | 0.14 | S1 |
| 0.42 | 440 | −0.04 | 0.73 | 0.24 | S2 |
| 0.45 | 386 | 0.01 | 0.67 | 0.26 | S3 |
| 0.37 | 193 | 0.01 | 1.24 | 0.25 | S4 |
| 0.35 | - | 0.96 | 1.08 | 0.11 | D |

IS is the isomer chemical shift, H is the hyperfine field on the iron nucleus, QS is the quadrupole splitting, W34 is the width of 3–4 lines of the inner sextets, and A is the fractional site population.

In studying polysaccharide-coated MNPs, Fourier-transform infrared (FTIR) spectroscopy is used, since the presence of a matrix does not prevent obtaining information about a particle and, in addition, makes it possible to establish changes in all main types of bonds between coating molecules.

The qualitative analysis of the spectra of starch and starch-MNPs allowed us to determine the main characteristic frequencies (Table 2). Figure 3 shows the FTIR spectra of the investigated samples. It can be seen that the spectra are different. It should be noted that the FTIR spectra of MNP-containing composites have a characteristic background increase in the region of 2000–4000 $cm^{-1}$. In the spectrum presented in Figure 3b, bonds in the region of 1200–1500 $cm^{-1}$ disappear, while bonds in the region of 800–1200 $cm^{-1}$ and hydroxyl ones remain unchanged.

According to the data of the spectral analysis, the absorption peaks at 388 and 570 $cm^{-1}$ in the spectrum of starch-MNPs correspond to O–Fe–O bending vibrations and Fe–O stretching modes and the starch chemisorption occurs on the nanoparticle surface through acetal bonds [27–29].

To determine the magnetic characteristics (magnetization, coercivity, and blocking temperature) of the synthesized nanoparticles, the hysteresis loops were measured in fields from −2 to 2 kOe at temperatures of 80–295 K. The saturation magnetization at room temperature was found to be 29.8 emu/g.

Figure 4a shows the hysteresis loops. The temperature dependence of the coercivity shown in Figure 4b obeys Equation (2), i.e., the coercivity decreases with an increase in temperature up to the blocking point [30]. This equation is conventionally used to describe single-domain noninteracting nanoparticles at temperatures below the blocking point [15,31,32]:

$$H_c(T) = H_c(0) \cdot (1 - (T/T_B)^{\alpha}). \quad (2)$$

**Table 2.** Absorption peaks and their interpretation ($cm^{-1}$).

| Range | Absorption Peak, Starch | Absorption Peak, Starch-MNPs | Description |
|---|---|---|---|
| 380–800 | | 388 | O–Fe–O |
| | 413 | | Vibrations of the pyranose ring and δ-hydroxyl groups |
| | 432 | | |
| | 487 | | |
| | 527 | | |
| | 573 | | Vibrations of the chain C–C–C . . . – Fe–O |
| | | 570 | |
| | 617 | | Vibrations of the pyranose ring and δ-hydroxyl groups |
| | 706 | | |
| | 767 | | |
| 800–1000 | 855 | | C–O in C–O–H |
| | | 866 | |
| | 922 | 900 | |
| 1000–1200 | 1001 | | C–O stretching of internal vibrations of C–O bonds (the bands characteristic of polysaccharides are caused by the presence of acetal bonds) |
| | | 1025 | |
| | 1075 | | |
| | | 1092 | |
| | | 1150 | |
| | 1161 | | |
| 1200–1500 | 1238 | | δ-$CH_2$ groups in $CH_2OH$ |
| | 1341 | | δ-O–H bonds in $CH_2OH$ |
| | 1368 | | δ-bonds of $CH_2$ groups |
| | 1421 | | δ-$CH_2$ groups |
| | 1461 | | δ-OH |
| 1500–2000 | 1654 | 1635 | δ-bonds in H–O–H (adsorbed water) |
| 2000–3000 | 2060 | | ν-bonds in CH and $CH_2$ groups |
| | 2153 | | |
| | 2890 | | |
| | 2930 | 2928 | C–H |
| 3000–4000 | 3406 | 3413 | Internal vibrations of OH groups involved in intermolecular and intramolecular H bonds |

Figure 4b shows, along with the temperature dependence of the coercivity, the fitting of the experimental data with Equation (2). The best fit parameters are $H_c(0) = 173$ Oe, $T_B = 377$ K, and $\alpha = 0.67$.

The blocking temperature can also be estimated using Néel-Brown formula (1). Assuming the anisotropy constant to be $4 \times 10^5$ erg/$cm^3$ [33] and the particle size to be ~11.5 ± 3 nm (according to the TEM data), we obtain that the blocking temperature of a nanoparticle, depending on its size, is 70–390 K.

Thus, according to the data obtained by the two methods, the average blocking temperature of the starch-MNPs is similar to room temperature and therefore they can be used in magnetic separation.

### *2.2. The Use of Starch-MNPs for One-Step Affine Purification of the MBP-Fused Recombinant Proteins*

The obtained starch-MNPs were tested as affine sorbents for purification of several recombinant hybrid proteins: MBP–cTnI, MBP–Surv, and MBP–MIA consisting of maltose-binding protein (MBP), cardiac troponin I (cTnI, 23.9 kDa), survivin (Surv, 16.5 kDa), and melanoma inhibitory activity protein (MIA, 12.1 kDa), respectively. As was mentioned above, MBP is widely used as an expression tag for producing recombinant proteins in bacterial cells. MBP as an auxiliary polypeptide increases the expression level of a target protein, improving the solubility and folding of the latter [20] and providing its one-step purification on amylose resin. Purification of the MBP-fusion protein exploits the natural

affinity of MBP for α-(1–4) maltodextrin with the micromolar dissociation constants [34]. The protein domains were linked by the ENLYFQS peptide, a specific protease site of the tobacco etch virus (TEV protease site). With this protease, the auxiliary polypeptide can be selectively removed, if desired. The target proteins chosen in this work are of considerable interest for medical diagnostics. Cardiac troponin I is a highly specific early biomarker for acute myocardial infarction. The MIA protein was identified as a key molecule involved in progression and metastasis of malignant melanomas. Survivin known as a baculoviral inhibitor of apoptosis repeat-containing 5 (BIRC5) is a member of the inhibitor of apoptosis protein (IAP) family, which inhibits caspases and blocks cell death. It is highly expressed in cancer and associated with a poorer clinical outcome.

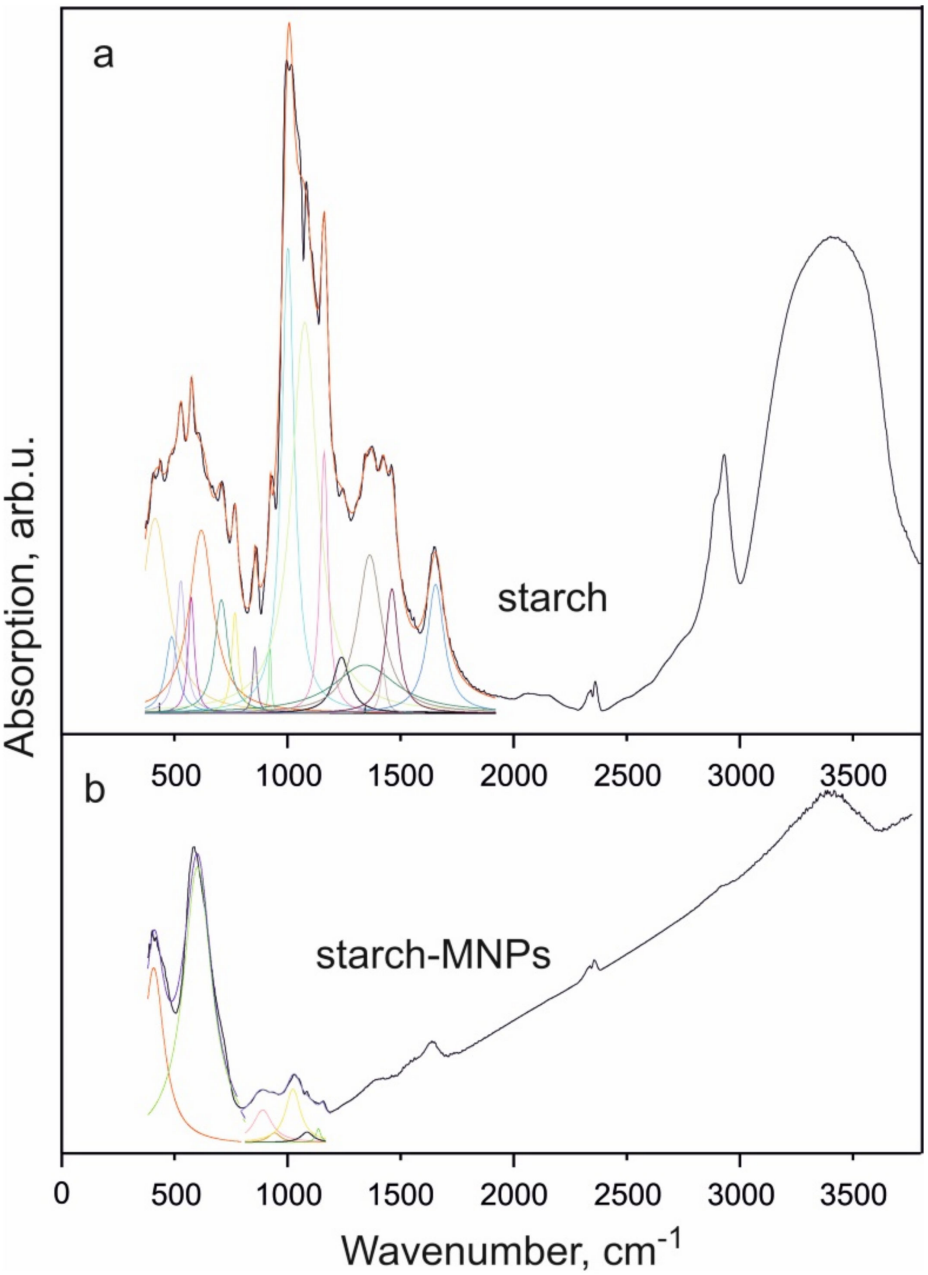


**Figure 3.** (**a**) FTIR spectrum of starch at $T$ = 300 K and division of the spectral region at 380–1900 $cm^{-1}$ into components. (**b**) FTIR spectrum of starch-MNPs and division of the spectral region at 380–1200 $cm^{-1}$ into components.

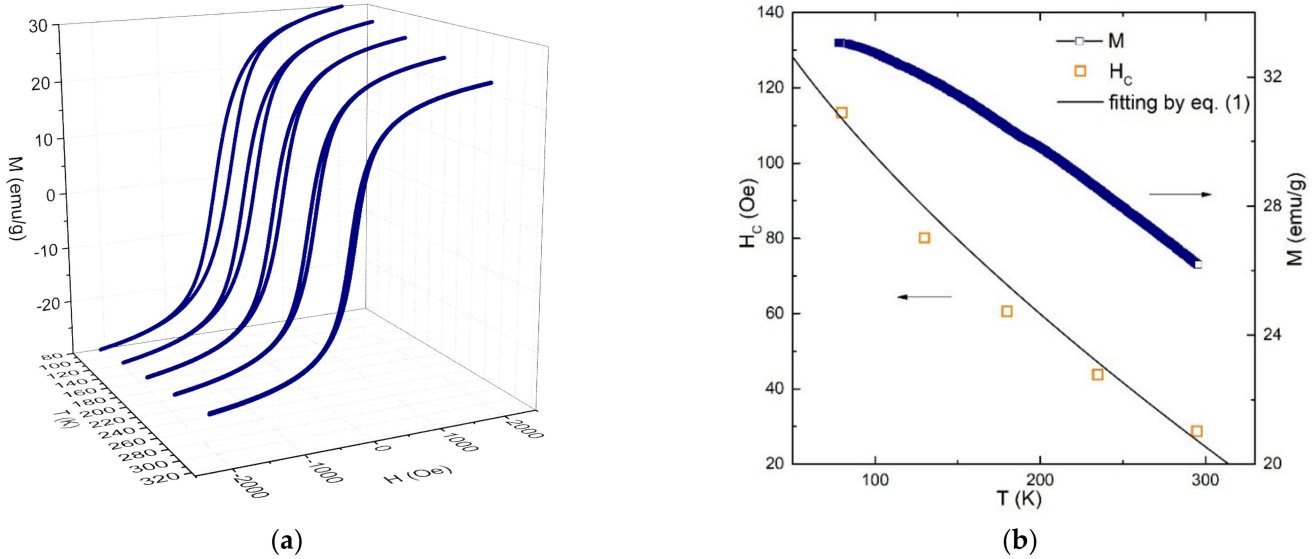


**Figure 4.** (**a**) Hysteresis loops measured in fields from –2 to 2 kOe in the temperature range of 80–295 K. (**b**) Temperature dependence of the coercivity (orange squares) fitted by Equation (2) (black line) and temperature dependence of magnetization measured in a field of 5 kOe (blue squares).

All the hybrid proteins were synthesized in the corresponding recombinant *E. coli* cells and, after ultrasonic disintegration, extracted from the cytoplasmic fraction. The proteins of interest were purified using a simple procedure, which does not require complex high-tech chromatographic equipment (see the detailed description in Section 3).

The purification process was controlled by sodium dodecyl sulfate–polyacrylamide gel electrophoresis (SDS-PAGE) (Figure 5). After washing off non-adsorbed proteins, the target proteins were efficiently eluted with 10 mM of maltose. It can be seen that, after one-step purification by starch-MNPs, the final protein samples had a purity of 80–94% (lanes 4 in Figure 5).

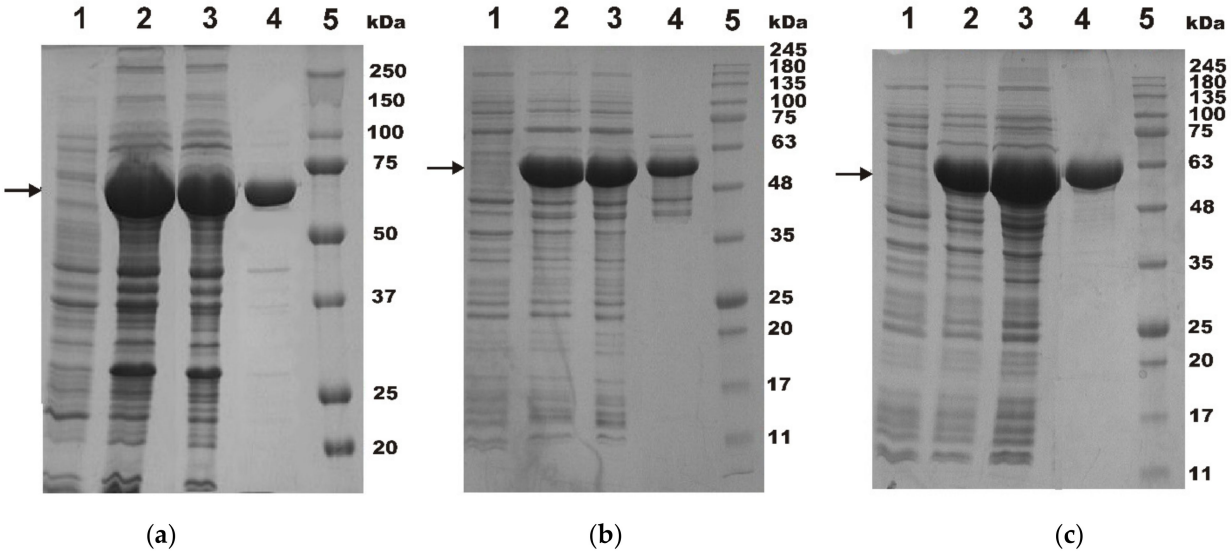


**Figure 5.** 12.5% SDS-PAGE analysis of MBP-TnI (**a**), MBP-MIA (**b**) and MBP-Surv (**c**) purification using starch-MNPs. Lanes: 1—whole-cells lysates before IPTG induction; 2—whole-cell lysates after IPTG induction; 3—cytoplasmic fraction; 4—fractions after elution by 10 mM maltose; 5—standard proteins (BioRad, Hercules, CA, USA), molecular weights are shown with numbers. Arrows show hybrid proteins bands.

It was found that the total amount of the protein taken for chromatography and summed up from all the eluted fractions was almost the same. This points out the absence of protein loss caused by the nonspecific irreversible adsorption on starch-MNPs.

The binding capacities were found to be 100.5 ± 5.1 μg for MBP-cTnI, 177 ± 14.1 μg for MBP–MIA, and 587.2 ± 52.2 μg for MBP–Surv (per milligram of starch-MNPs). These values exceed the parameters of commercial amylose magnetic beads (the binding capacity of MBP5*-paromyosin ΔSal fusion protein is 10 μg per milligram of New England Biolabs amylose magnetic beads) and those of amylose-coated particles obtained by Lim et al. [35] (the binding capacity of GFP fused with MBP is 72 μg per milligram of particles).

Several experiments on changing the starch-MNP capacity were carried out. This parameter was found to be independent of the concentration of starch used in co-precipitation within 5–50 g/L (the data are not shown). In all the purification experiments, the nanoparticles prepared at a starch concentration of 20 g/L were used.

To evaluate the synthesis reproducibility, we obtained three starch-MNP samples in parallel experiments and tested them in the MBP–cTnI purification. The high-purity MBP-cTnI yields were found to be similar, with a variation coefficient of 14.2%.

The recycling property of starch-MNPs was evaluated by measuring the MBP-binding capacity after three cycles of their use. MBP-cTnI was purified for three times using the same starch-MNPs sample (see Section 3). The particles showed a remarkable reuse robustness: the purified MBP-cTnI yields were 94.7, 104.1, and 102.8 μg per milligram of starch-MNPs after the first, second, and third cycle, respectively. Thus, the MBP binding capacity of starch-MNPs remains unchanged after the three cycles of reuse. It is noteworthy that, in principle, due to the low cost of the synthesized particles, this material can be disposable.

The storage of starch-MNPs in distilled water without preservatives leads to the complete loss of the MBP binding capacity in three weeks. It was found, however, that the initial binding capacity can be kept for up to six months by adding 0.05% of $NaN_3$.

## 3. Materials and Methods

### 3.1. Synthesis and Characterization of Nanoparticles

Iron oxide nanoparticles were prepared by co-precipitation from a solution containing 20 g/L of ammonium iron (II) sulfate, 0.2–0.4 M of sodium citrate, 20 g/L of EDTA-$Na_2$, and 20 g/L of cornstarch. At a temperature of 80 °C, this solution was added with a 0.1 M of the sodium hydroxide solution until neutral pH. The starch-MNPs were thoroughly washed with distilled water to remove ions and stored with the 0.05% aqueous solution of $NaN_3$.

The electron microscopy study was carried out on a Hitachi HT7700 transmission electron microscope at an accelerating voltage of 100 kV at the Krasnoyarsk Regional Center for Collective Use of the Krasnoyarsk Scientific Center, Siberian Branch of the Russian Academy of Sciences. Mössbauer spectra were recorded on an MS-1104Em spectrometer with a 57Co(Cr) source at room temperature. Isomer chemical shifts were referenced to α-Fe. IR absorption spectra were recorded on a Bruker VERTEX-80V vacuum FTIR spectrometer in the range of 380–7500 $cm^{-1}$. The samples were pressed tablets with potassium bromide with a diameter of 13 mm and a thickness of ~0.55 mm. They were carefully ground with 0.2 g of KBr in a ratio of 2:100 in a mortar. The spectra were obtained using a Globar light source (a U-shaped silicon carbide arc), an RT-DLaTGS detector, and a KBr beam splitter. The experimental data were processed and analyzed using the OriginPro software (OriginPro 2015, OriginLab Corporation, Northampton, MA, USA). The static magnetic measurements were performed on an automated vibrating sample magnetometer in fields of up to 15 kOe at room temperature [36].

### 3.2. MBP Hybrid Protein Expression

The sequences of genes encoding human surviving, cardiac troponin I, and MIA optimized for bacterial expression (Evrogen, Moscow, Russia) [37], were cloned into the pMALc5x vector.

*E. coli* BL21-CodonPlus (DE3)-RIPL cells (Stratagene, La Jolla, CA, USA) transformed by the corresponding plasmid were cultivated in an LB medium containing 2 g/L of glucose and 200 μg/mL of ampicillin at 37 °C until the culture reached an $OD_{600}$ of 0.5–0.7; then, 0.33 mM of IPTG was added and the cultivation was continued at 37 °C for 3 h. The cells were harvested by centrifugation, the pellet was resuspended in buffer A (20 mM Tris-HCl pH 7.5, 0.2 M NaCl, 1 mM EDTA) in a ratio of 1:5 (*w*/*v*), disrupted by sonication (20 s × 6) at 0 °C, and the mixture was centrifuged. The pellet was discarded and the supernatant was used in the further protein purification experiments.

### *3.3. MBP Hybrid Proteins Purification by the Magnetic Nanoparticles*

The cell lysate supernatant (800 μL aliquots) was mixed with 500 μL of the starch-MNP suspension at 4 °C for 1 h under shaking. Then, the particles were fixed at the bottom with a magnet and the solution was removed. The particles were washed with 3 portions of buffer A (1 mL) and then the hybrid proteins were eluted with 800 μL of the elution buffer (10 mM of maltose in buffer A).

The purity of the protein samples was controlled by Laemmli electrophoresis. The protein concentration was measured using a Bio-Rad DCTM protein assay kit.

### *3.4. Starch-MNPs Recycling*

Recycling of starch-MNPs was evaluated by quantifying the purified MBP-cTnI capacity for three additional loading cycles with 0.8 mL of cell lysate to 0.5 mL of the starch-MNP suspension. After the MBP-cTnI binding and elution (as described above), the starch-MNPs were regenerated by washing with the elution buffer for several times followed by re-equilibration with buffer A. Then, the cycle of regeneration, re-equilibration, binding, washing, and elution was repeated. These experiments were carried out for three times.

## 4. Conclusions

It was shown that starch-coated magnetic iron oxide nanoparticles synthesized by a simple and cost-effective co-precipitation method with cornstarch as a stabilizing agent represent a high binding affinity material that can ensure the high-efficiency purification of a recombinant protein bearing the maltose-binding protein as an auxiliary fragment. Starch-MNPs in the form of cubic nanocrystals with an average size of ~11.5 nm were synthesized. It was demonstrated that the saturation magnetization (29.8 emu/g at room temperature) and blocking temperature similar to room temperature (377 K, according to the temperature dependence of the coercivity, or 70–390 K, according to the Néel-Brown equation) make these nanoparticles good candidates for use in magnetic separation. The FTIR spectroscopy data disclosed the formation of a bond between a nanoparticle and starch.

Starch-MNPs exhibit the high specificity and purification capacity for MBP-fusion proteins (100–500 μg per milligram of the particles), as well as the reusability without the binding capacity and protein purity loss. They provide the fast, convenient, specific, and cost-effective one-step purification of recombinant proteins. The use of magnetic separation in the purification process makes it possible to exclude the centrifugation and filtration stages, as well as the need for expensive chromatographic systems and columns.

Thus, the obtained starch-MNPs have a high potential for use in purification of recombinant proteins. In our opinion, this material has also good prospects as a basis for the development of specific biosensors. The proposed simple and cost-effective starch-MNP synthesis method can be easily implemented at non-specialized (resource-limited) laboratories and facilities.

**Author Contributions:** Conceptualization, V.V.K.; synthesis and characterization of starch-MNPs, R.N.Y.; study of starch-MNPs usage for affine purification of the recombinant proteins, A.N.K. and V.V.K.; IR measurements, Y.V.G.; VSM measurements, D.A.V.; Mössbauer spectroscopy measurements, O.A.B.; writing—original draft preparation, V.V.K. and R.N.Y.; writing—review and editing, S.V.S. and L.A.F.; supervision, S.V.S. and L.A.F.; funding acquisition, S.V.S. All authors have read and agreed to the published version of the manuscript.

**Funding:** This study was supported by the Russian Science Foundation and the Krasnoyarsk Territorial Foundation for Support of Scientific and R&D Acitvities, project No. 22-14-20020.

**Institutional Review Board Statement:** Not applicable.

**Informed Consent Statement:** Not applicable.

**Data Availability Statement:** Not applicable.

**Acknowledgments:** The HRTEM study was carried out on the equipment of the Krasnoyarsk Regional Center for Collective Use, Krasnoyarsk Scientific Center, Siberian Branch of the Russian Academy of Sciences. The authors are grateful to M.N. Volochaev for the HRTEM measurements.

**Conflicts of Interest:** The authors declare no conflict of interest.

## References

1. Kim, S.-E.; Tieu, M.V.; Hwang, S.Y.; Lee, M.-H. Magnetic particles: Their applications from sample preparations to biosensing platforms. *Micromachines* **2020**, *11*, 302. [CrossRef] [PubMed]
2. Stueber, D.D.; Villanova, J.; Aponte, I.; Xiao, Z.; Colvin, V.L. Magnetic Nanoparticles in Biology and Medicine: Past, Present, and Future Trends. *Pharmaceutics* **2021**, *13*, 943. [CrossRef] [PubMed]
3. Ma, Y.; Chen, T.; Iqbal, M.Z.; Yang, F.; Hampp, N.; Wu, A.; Luo, L. Applications of magnetic materials separation in biological nanomedicine. *Electrophoresis* **2019**, *40*, 2011–2028. [CrossRef] [PubMed]
4. Qian, B.; Zhao, Q.; Ye, X. Ultrasound and magnetic responsive drug delivery systems for cardiovascular application. *J. Cardiovasc. Pharmacol.* **2020**, *76*, 414–426. [CrossRef]
5. Zeng, L.; Wu, D.; Zou, R.; Chen, T.; Zhang, J.; Wu, A. Paramagnetic and superparamagnetic inorganic nanoparticles for T1-weighted magnetic resonance imaging. *Curr. Med. Chem.* **2018**, *25*, 2970–2986. [CrossRef] [PubMed]
6. Fatima, H.; Charinpanitkul, T.; Kim, K.-S. Fundamentals to apply magnetic nanoparticles for hyperthermia therapy. *Nanomaterials* **2021**, *11*, 1203. [CrossRef]
7. Masud, M.K.; Na, J.; Younus, M.; Hossain, M.S.A.; Bando, Y.; Shiddiky, M.J.A.; Yamauchi, Y. Superparamagnetic nanoarchitectures for disease-specific biomarker detection. *Chem. Soc. Rev.* **2019**, *48*, 5717–5751. [CrossRef]
8. Fatima, H.; Kim, K.-S. Magnetic nanoparticles for bioseparation. *Korean J. Chem. Eng.* **2017**, *34*, 589–599. [CrossRef]
9. Elahi, N.; Rizwan, M. Progress and prospects of magnetic iron oxide nanoparticles in biomedical applications: A review. *Artif. Organs* **2021**, *45*, 1272–1299. [CrossRef]
10. Concas, G.; Congiu, F.; Muscas, G.; Peddis, D. Determination of blocking temperature in magnetization and Mössbauer time scale: A functional form approach. *J. Phys. Chem. C* **2017**, *121*, 16541–16548. [CrossRef]
11. Khmelinskii, I.; Makarov, V.I. EPR hyperthermia of S. cerevisiae using superparamagnetic $Fe_3O_4$ nanoparticles. *J. Therm. Biol.* **2018**, *77*, 55–61. [CrossRef] [PubMed]
12. Lee, J.-H.; Kim, B.; Kim, Y.; Kim, S.-K. Ultra-high rate of temperature increment from superparamagnetic nanoparticles for highly efficient hyperthermia. *Sci. Rep.* **2021**, *11*, 4969. [CrossRef] [PubMed]
13. Bai, Y.; Cui, Y.; Paoli, G.C.; Shi, C.; Wang, D.; Zhou, M.; Zhang, L.; Shi, X. Synthesis of amino-rich silica-coated magnetic nanoparticles for the efficient capture of DNA for PCR. *Colloids Surf. B Biointerfaces* **2016**, *145*, 257–266. [CrossRef] [PubMed]
14. Tyumentseva, A.V.; Yaroslavtsev, R.N.; Stolyar, S.V.; Saitova, A.T.; Tyutrina, E.S.; Gorbenko, A.S.; Stolyar, M.A.; Olkhovskiy, I.A. Silica-coated iron oxide nanoparticles for DNA isolation for molecular genetic studies in hematology. *Genet. Test. Mol. Biomarkers* **2021**, *25*, 611–614. [CrossRef] [PubMed]
15. Komogortsev, S.V.; Stolyar, S.V.; Chekanova, L.A.; Yaroslavtsev, R.N.; Bayukov, O.A.; Velikanov, D.A.; Volochaev, M.N.; Eroshenko, P.E.; Iskhakov, R.S. Square plate shaped magnetite nanocrystals. *J. Magn. Magn. Mater.* **2021**, *527*, 167730. [CrossRef]
16. Assa, F.; Jafarizadeh-Malmiri, H.; Ajamein, H.; Vaghari, H.; Anarjan, N.; Ahmadi, O.; Berenjian, A. Chitosan magnetic nanoparticles for drug delivery systems. *Crit. Rev. Biotechnol.* **2017**, *37*, 492–509. [CrossRef]
17. Stolyar, S.V.; Krasitskaya, V.V.; Frank, L.A.; Yaroslavtsev, R.N.; Chekanova, L.A.; Gerasimova, Y.V.; Volochaev, M.N.; Bairmani, M.S.; Velikanov, D.A. Polysaccharide-coated iron oxide nanoparticles: Synthesis, properties, surface modification. *Mater. Lett.* **2021**, *284*, 128920. [CrossRef]
18. Kheilkordi, Z.; Mohammadi Ziarani, G.; Mohajer, F.; Badiei, A.; Sillanpää, M. Recent advances in the application of magnetic bio-polymers as catalysts in multicomponent reactions. *RSC Adv.* **2022**, *12*, 12672–12701. [CrossRef]
19. Duplay, P.; Bedouelle, H.; Fowler, A.; Zabin, I.; Saurin, W.; Hofnung, M. Sequences of the malE gene and of its product, the maltose-binding protein of Escherichia coli K12. *J. Biol. Chem.* **1984**, *259*, 10606–10613. [CrossRef]
20. Waugh, D.S. The remarkable solubility-enhancing power of Escherichia coli maltose-binding protein. *Postepy Biochem.* **2016**, *62*, 377–382. [CrossRef]
21. Duong-Ly, K.C.; Gabelli, S.B. Affinity purification of a recombinant protein expressed as a fusion with the maltose-binding protein (MBP) tag. *Methods Enzymol.* **2015**, *559*, 17–26. [PubMed]

22. Kobashigawa, Y.; Namikawa, M.; Sekiguchi, M.; Inada, Y.; Yamauchi, S.; Kimoto, Y.; Okazaki, K.; Toyota, Y.; Sato, T.; Morioka, H. Expression, purification and characterization of CAR/NCOA-1 tethered protein in E. coli using maltose-binding protein fusion tag and gelatinized corn starch. *Biol. Pharm. Bull.* **2021**, *44*, 125–130. [CrossRef] [PubMed]
23. Huang, Y.C.; Chang, H.H.; Mou, Y.; Chi, P.; Chan, J.C.; Luo, S.C. Purification of recombinant nacre-associated mineralization protein AP7 fused with maltose-binding protein. *Protein Expr. Purif.* **2014**, *100*, 26–32. [CrossRef] [PubMed]
24. Park, K.C.; Gaze, D.C.; Collinson, P.O.; Marber, M.S. Cardiac troponins: From myocardial infarction to chronic disease. *Cardiovasc. Res.* **2017**, *113*, 1708–1718. [CrossRef]
25. Gunaldi, M.; Isiksacan, N.; Kocoglu, H.; Okuturlar, Y.; Gunaldi, O.; Topcu, T.; Karabulut, M. The value of serum survivin level in early diagnosis of cancer. *J. Cancer Res. Ther.* **2018**, *14*, 570–573. [PubMed]
26. Riechers, A.; Bosserhoff, A.K. Melanoma inhibitory activity in melanoma diagnostics and therapy—A small protein is looming large. *Exp. Dermatol.* **2014**, *23*, 12–14. [CrossRef] [PubMed]
27. Wei, Y.; Han, B.; Hu, X.; Lin, Y.; Wang, X.; Deng, X. Synthesis of $Fe_3O_4$ nanoparticles and their magnetic properties. *Procedia Eng.* **2012**, *27*, 632–637. [CrossRef]
28. Asgari, S.; Fakhari, Z.; Berijani, S. Synthesis and characterization of $Fe_3O_4$ magnetic nanoparticles coated with carboxymethyl chitosan grafted sodium methacrylate. *J. Nanostructures* **2014**, *4*, 55–63.
29. Shah, N.; Ahmad, H.; Shah, S.S.; Khan, I. Synthesis and characterization of starch coated natural magnetic iron oxide nanoparticles for the removal of methyl orange dye from water. *Lett. Appl. NanoBioScience* **2021**, *10*, 2750–2759.
30. Pfeiffer, H. Determination of anisotropy field distribution in particle assemblies taking into account thermal fluctuations. *Phys. Status Solidi* **1990**, *118*, 295–306. [CrossRef]
31. Iskhakov, R.S.; Komogortsev, S.V.; Stolyar, S.V.; Prokof'ev, D.E.; Zhigalov, V.S. Structure and magnetic properties of nanocrystalline condensates of iron obtained by pulse plasma evaporation. *Phys. Met. Metallogr.* **1999**, *88*, 261–269.
32. Komogortsev, S.V.; Iskhakov, R.S.; Balaev, A.D.; Okotrub, A.V.; Kudashov, A.G.; Momot, N.A.; Smirnov, S.I. Influence of the inhomogeneity of local magnetic parameters on the curves of magnetization in an ensemble of $Fe_3C$ ferromagnetic nanoparticles encapsulated in carbon nanotubes. *Phys. Solid State* **2009**, *51*, 2286. [CrossRef]
33. Pisane, K.L.; Singh, S.; Seehra, M.S. Unusual enhancement of effective magnetic anisotropy with decreasing particle size in maghemite nanoparticles. *Appl. Phys. Lett.* **2017**, *110*, 222409. [CrossRef]
34. Miller, D.M.; Olson, J.S.; Pflugrath, J.W.; Quiocho, F.A. Rates of ligand binding to periplasmic proteins involved in bacterial transport and chemotaxis. *J. Biol. Chem.* **1983**, *258*, 13665–13672. [CrossRef]
35. Lim, M.-C.; Lee, G.-H.; Huynh, D.T.N.; Letona, C.A.M.; Seo, D.-H.; Park, C.-S.; Kim, Y.-R. Amylosucrase-mediated synthesis and self-assembly of amylose magnetic microparticles. *RSC Adv.* **2015**, *5*, 36088. [CrossRef]
36. Velikanov, D.A. Vibration Magnetic Meter. RF Patent for the Invention RU2341810 (C1), 20 December 2008. Bulletin No. 3..
37. Krasitskaya, V.V.; Bashmakova, E.E.; Kudryavtsev, A.N.; Vorobyeva, M.A.; Shatunova, E.A.; Frank, L.A. The hybrid protein ZZ–OL as an analytical tool for biotechnology research. *Russ. J. Bioorganic Chem.* **2020**, *46*, 1004–1010. [CrossRef]